SCIENTIFIC REPORTS

OPEN

SUBJECT AREAS:
CHEMICAL ENGINEERING
MEDICAL RESEARCH

Received
16 June 2014

Accepted
12 September 2014

Published
10 October 2014

Correspondence and requests for materials should be addressed to D.S. (denis.spitzer@isl.eu)

Continuous engineering of nano-cocrystals for medical and energetic applications

D. Spitzer, B. Risse, F. Schnell, V. Pichot, M. Klaumünzer & M. R. Schaefer

NS3E, ISL-CNRS-UdS (Nanomatériaux pour les Systèmes Sous Sollicitations Extrêmes) UMR 3208, French-German Research Institute of Saint-Louis, 5, rue du Général Cassagnou, B.P. 70034, 68301 St Louis, France.

Cocrystals, solid mixtures of different molecules on molecular scale, are supposed to be tailor made materials with improved employability compared to their pristine individual components in domains such as medicine and explosives. In medicine, cocrystals are obtained by crystallization of active pharmaceutical ingredients with precisely chosen coformers to design medicaments that demonstrate enhanced stability, high solubility, and therefore high bioavailability and optimized drug up-take. Nanoscaling may further advance these characteristica compared to their micronsized counterparts – because of a larger surface to volume ratio of nanoparticles. In the field of energetic materials, cocrystals offer the opportunity to design smart explosives, combining high reactivity with significantly reduced sensitivity, nowadays essential for a safe manipulation and handling. Furthermore, cocrystals are used in ferroelectrics, non-linear material response and electronic organics. However, state of the art batch processes produce low volume of cocrystals of variable quality and only have produced micronsized cocrystals so far, no nano-cocrystals. Here we demonstrate the continuous preparation of pharmaceutical and energetic micro- and nano-cocrystals using the Spray Flash Evaporation process. Our laboratory scale pilot plant continuously prepared up to 8 grams per hour of Caffeine/Oxalic acid 2 : 1, Caffeine/Glutaric acid 1 : 1, TNT/CL-20 1 : 1 and HMX/Cl-20 1 : 2 nano- and submicronsized cocrystals.

Cocrystals are built up from several types of molecular interactions: hydrogen bonds, ionic bonds, π-π stacking and van der Waals forces[1–4]. It has been demonstrated that cocrystals are thermodynamically more stable than crystals of pristine compounds[5]. For pharmaceutical applications, cocrystallization is highly promising for tailoring properties of the Active Pharmaceutical Ingredient (API) and coformer couple to improve dissolution kinetics, the degree of bioavailability, and also the stability (pH and thermal) of the compound[1,3–6].

Caffeine, well known as a nervous system stimulant and a smooth muscle relaxant, is generally used as a formulation additive to analgesic remedies[8]. The advantages of cocrystallization are described, for example, on this pharmaceutical compound, which is able to cocrystallize with several compounds such as carboxylic acids, resulting in an increased stability to humidity. Whereas the cocrystal based on caffeine and glutaric acid is partially unstable to humidity[7], cocrystals obtained with oxalic acid exhibit complete stability to humidity over a period of several weeks[8].

In the field of explosive molecules - some of which are also employed as pharmaceutical substances[9] - the reactive properties strongly correlate to inherent parameters as the degree of proximity between the oxidative and fuel parts within the explosive molecule. Although the research on new explosive molecules is still going on for increasing performance and security, the nano-structuring and nano-cocrystallization of existing explosive mixtures offer promising opportunities to enhance stability against unwanted decomposition and therefore safety of these advanced materials[2,10–18]. Recently, it has been shown that the equimolar cocrystallization of 2,4,6-trinitrotoluene (TNT) with 2,4,6,8,10,12-hexanitro-2,4,6,8,10,12-hexaazaiso-wurtzitane (CL-20), TNT/CL-20, leads to an explosive cocrystal with reduced sensitivity compared to the one of the powerful pure CL-20 compound[2]. From an energetic point of view, more interesting is the cocrystallization of 1,3,5,7-tetranitro-1,3,5,7-tetrazacyclooctane (HMX) with 2,4,6,8,10,12-hexanitro-2,4,6,8,10,12-hexaazaiso-wurtzitane (CL-20), HMX/CL-20 1 : 2 molar ratio, leading to an explosive cocrystal with a predicted detonation velocity

of 100 m/s higher than that of beta-HMX and with a reduced sensitivity similar to that of HMX but far away from the high sensitivity of pure CL-20[13].

At the moment, four different main techniques contribute to the state of the art in preparation of cocrystals[1]. All comprise crystallization by slow evaporation of concentrated solutions, solid-state grinding of the reactants in presence (or not) of a solvent, electrochemically induced reactions and the kinetically controlled crystallization by rapid evaporation of the solvent from a solution containing single pure compounds. In fact, it must be stressed that this last dynamic technique enables the formation of metastable polymorphs, not accessible by classical crystallization techniques. However, as these four techniques allow synthesizing products by a discontinuous manner, they are not suitable for high industrial productions. A further drawback, these processes have in common, is the formation of only micronsized cocrystals, with lower bioavailability due to the slower dissolution rate compared to nanomaterials. The Rapid Expansion of Supercritical Solutions (RESS) process was developed to elaborate nanoexplosives. This specific technique also offers some cons: the use of supercritical carbon dioxide as a poor solvent considerably reduces the production capacity. Furthermore, it is not possible to control precisely solute concentrations, which is, however, essential for cocrystals as they are based on defined molecular ratios between the individual pristine compounds[19].

By means of the Spray Flash Evaporation process[20–22], depending on the type of molecular interaction (see above) between the different molecules, different types of mixtures can be engineered (Fig. 1), such as entirely crystalline composites, semi-crystalline mixtures and cocrystals. Single molecules that are not subject to these molecular interactions are not to be expected to effectively form cocrystals or related material. In Addition intermolecular steric hindrance can prevent cocrystallization.

The Flash Evaporation technique is characterized by an extraordinary fast crystallization rate compared to other classical techniques, that favors close interaction between different molecules to produce desired cocrystals.

Results and Discussion

To demonstrate feasibility of this concept for pharmaceutical applications, two model caffeine based cocrystal systems were chosen: Caffeine/Oxalic acid 2 : 1 and Caffeine/Glutaric acid 1 : 1 cocrystals (both molar ratio).

For the domain of explosives, we have elaborated two nanococrystal systems and two semi-crystalline nanocomposites. Synthesized nano-cocrystal systems are 2,4,6-trinitrotoluene (TNT)/2,4,6,8,10,12-hexanitro-2,4,6,8,10,12-hexaazaiso-wurtzitane (CL-20) 1 : 1, named as TNT/CL-20 1 : 1, and 1,3,5,7-tetranitro-1,3,5,7-tetrazacyclooctane (HMX)/2,4,6,8,10,12-hexanitro-2,4,6,8,10,12-hexaazaiso-wurtzitane (CL-20), named as HMX/CL-20 1 : 2. Semi-crystalline nanocomposites of TNT and HMX were crystallized in 1 : 1 and 1 : 2 molar ratios, named as TNT/HMX 1 : 1 and TNT/HMX 1 : 2, respectively. Chemical formulae of pure compounds are depicted in Figure 2h.

Our products were observed by Atomic Force Microscopy (AFM) at room temperature and atmospheric pressure. In contrast with electron microcopy, the mild measuring conditions do not destroy nor alter morphology of the sample. Based on our results of AFM imaging, particle size distributions of corresponding mixtures were determined (Fig. 2g).

For the cocrystals, mean particle size ranges from $x_{mean} = 59$ nm (HMX/CL-20 1 : 2) to $x_{mean} = 111$ nm (Caffeine/Glutaric acid 1 : 1). In case of the Caffeine/Glutaric acid 1 : 1 cocrystal, the formation of a more pronounced acicular shape by trend was observed (Fig 2b) – in contrast to primarily spherical morphologies of the alternative systems (Fig 2a, c–f.). The smallest particles were found in both TNT/HMX mixtures with a mean particle size of $x_{mean} \sim 40$ nm for each (Fig 2g).

In order to prove the formation of cocrystals, X-ray diffraction (XRD) in the range of $2\theta = 10$ to 35 was performed on every sample (Fig. 3): As can be seen from Caffeine/Oxalic acid 2 : 1, Caffeine/Glutaric acid 1 : 1, TNT/CL-20 1 : 1, and HMX/CL-20 1 : 2 -XRD-patterns, mixtures significantly differ from those of individual pristine substances. This fact clearly confirms cocrystallization of individual substances. All obtained diffraction patterns correspond to theoretical patterns of cocrystals taken from Cambridge Structural Database, and to those described in literature[2,8,13]. Presented XRD-patterns are in fine agreement with the results given by Bolton and Matzger who present XRD-data of micronsized cocrystals of TNT/CL-20 1 : 1 and of HMX/CL-20 1 : 2[2,13]. They claim intrinsic propagating hydrogen bonding and non propagating nitro-aromatic and nitro-nitro interactions between the TNT molecule and the CL-20 molecule to build up the cocrystal[2]. In case of HMX/CL-20 1 : 2, the crystal structure features a packing motif in which layers of HMX alternate with bilayers of CL-20[13]. Finally, mainly mono-cocrystals at the nanoscale were formed as the mean particle size of 60 nm given by AFM is close to the mean coherent crystallite size of 62 nm derived from the full width at half maximum (FWHM) of the X-ray signals (determined by the

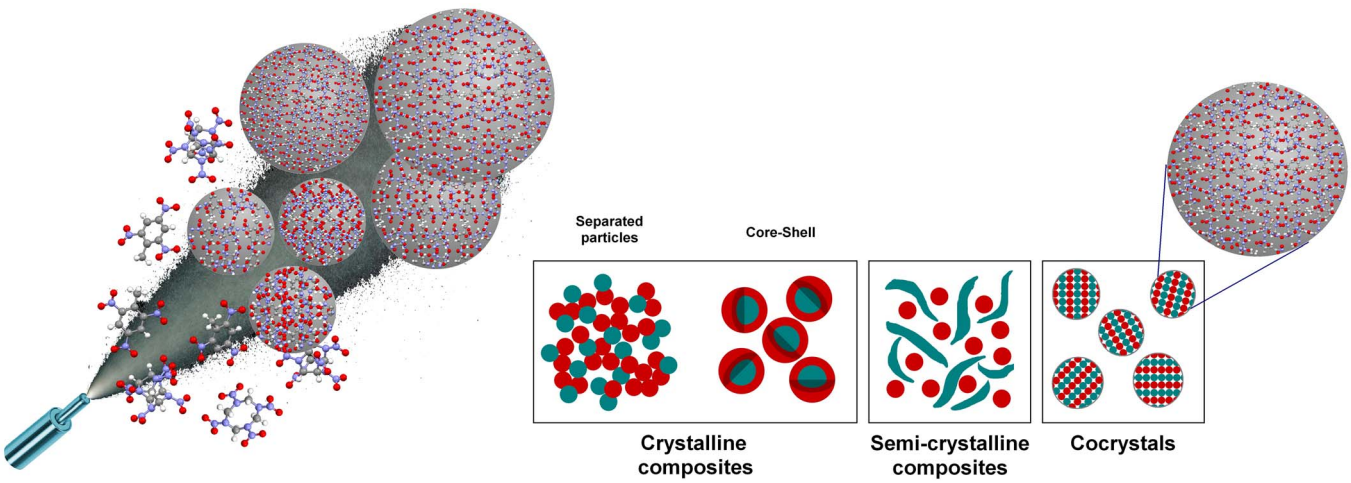

Figure 1 | Process scheme, and types of organic mixtures obtained by the Spray Flash Evaporation Process. Drawing created by the authors, software: Mercury 3.1, Gimp 2.8, Inkscape 0.48.5 and Paint 6.3.

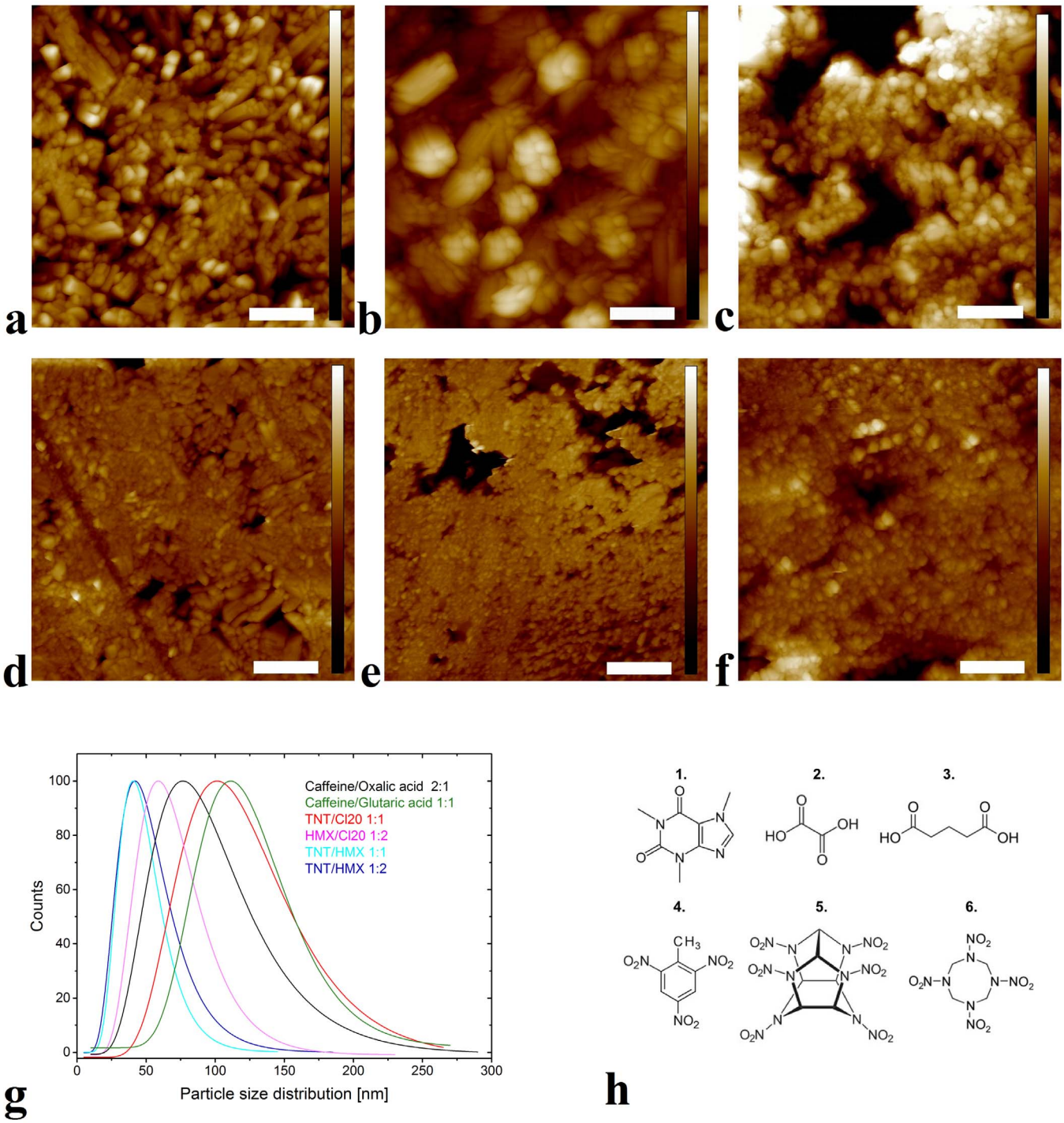

Figure 2 | AFM topography, particle size distributions and molecules of the pure compounds. (a), Caffeine/Oxalic acid 2 : 1, (b), Caffeine/Glutaric acid 1 : 1, (c), TNT/CL-20 1 : 1, (d), HMX/CL-20 1 : 2, (e), TNT/HMX 1 : 1, (f), TNT/HMX 1 : 2, a-f, lateral scale bars, 1 μm, height scale bars, 0,4 μm, (g), particle size distributions of the cocrystals and semi-crystalline mixtures and (h), chemical formulae of the pure compounds (**1.** Caffeine, **2.** Oxalic acid, **3.** Glutaric acid, **4.** TNT, **5.** CL-20, **6.** HMX).

well known Scherrer equation). For all other cocrystals, measured particle sizes were approximately two or three times larger than the specific corresponding coherent crystallite size, showing that synthesized nanoparticles are polycrystalline and composed of five to ten single crystal domains.

In case of TNT/HMX 1 : 1 and 1 : 2 formulations, the XRD pattern of the pristine TNT was still present in both mixtures whereas only the strongest peaks of HMX could be found near the baseline. The latter indicates that cocrystals were not formed. Moreover, the lack of HMX signals indicates that this pure compound is rather present in an amorphous state, which indicates semi-crystalline nature of these systems that are physically mixed, not chemically combined via molecular interactions inside of a cocrystal. XRD analyses performed after ageing for a period of two months of the product show that no crystallization of HMX occurs and that it remains in an amorphous state, making this composition a mixture of crys-

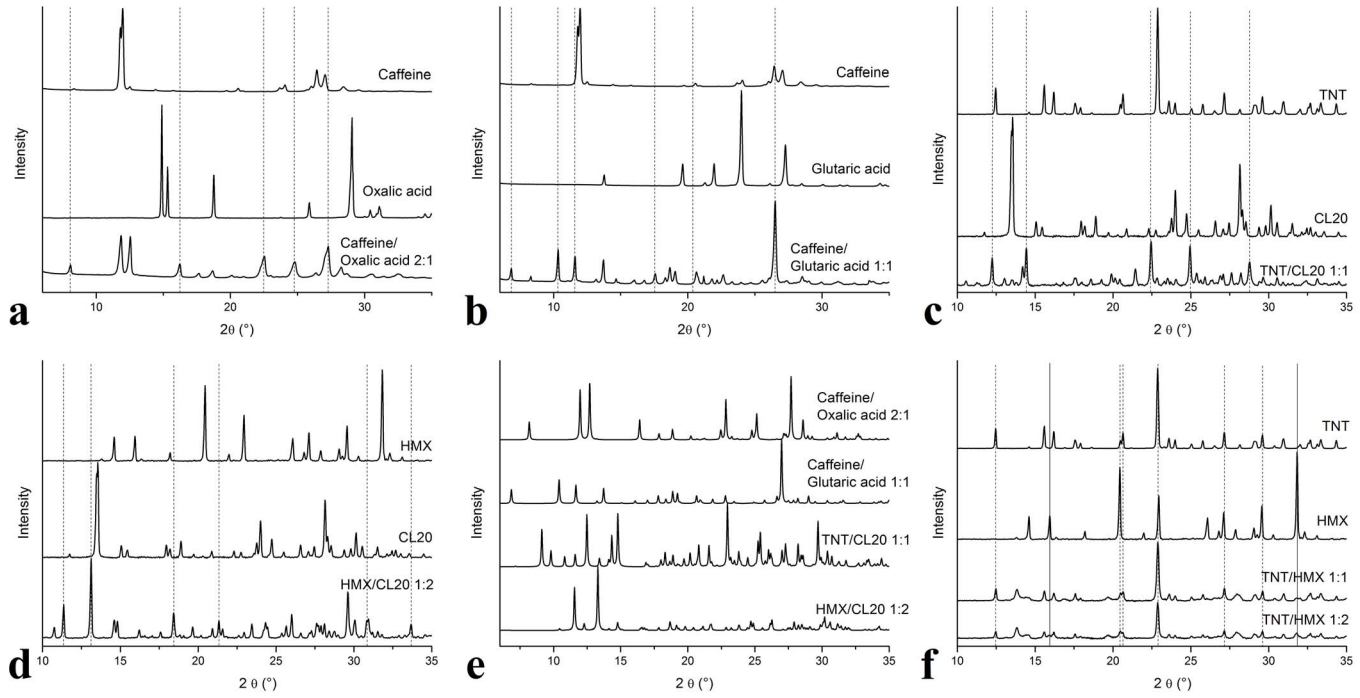

Figure 3 | **XRD Powder diffractograms.** (a), Caffeine/Oxalic acid 2 : 1, (b), Caffeine/Glutaric acid 1 : 1, (c), TNT/CL-20 1 : 1, (d), HMX/CL-20 1 : 2, (e), theoretical diffraction patterns of the cocrystals (Cambridge Structural Database), and (f), TNT/HMX semi-crystalline mixtures.

talline TNT and amorphous HMX. Moreover, the small particle size observed by AFM (see Fig 2g) is explained by the inability to grow large cocrystals and by mutually hindered growth of TNT and HMX pure particles.

Thermal behavior of the as-synthesized cocrystals was studied using Differential Scanning Calorimetry (DSC). As shown in Figure 4, the presence of TNT/CL-20 1 : 1 cocrystal is obvious. This is evidenced during the first heating by the lack of the characteristic pure TNT melting signal at 80°C (Fig. 4a). This indicates that TNT and CL-20 molecules form a well-defined cocrystal lattice instead of two different crystalline phases. The observed endothermic signal at 135°C (onset temperature) was considered as the melting temperature of the cocrystal. After the first heating phase the DSC crucible was cooled down and heated again. During the second heating, the melting signal of pure TNT appeared as expected at 80°C. This experiment definitely demonstrates the

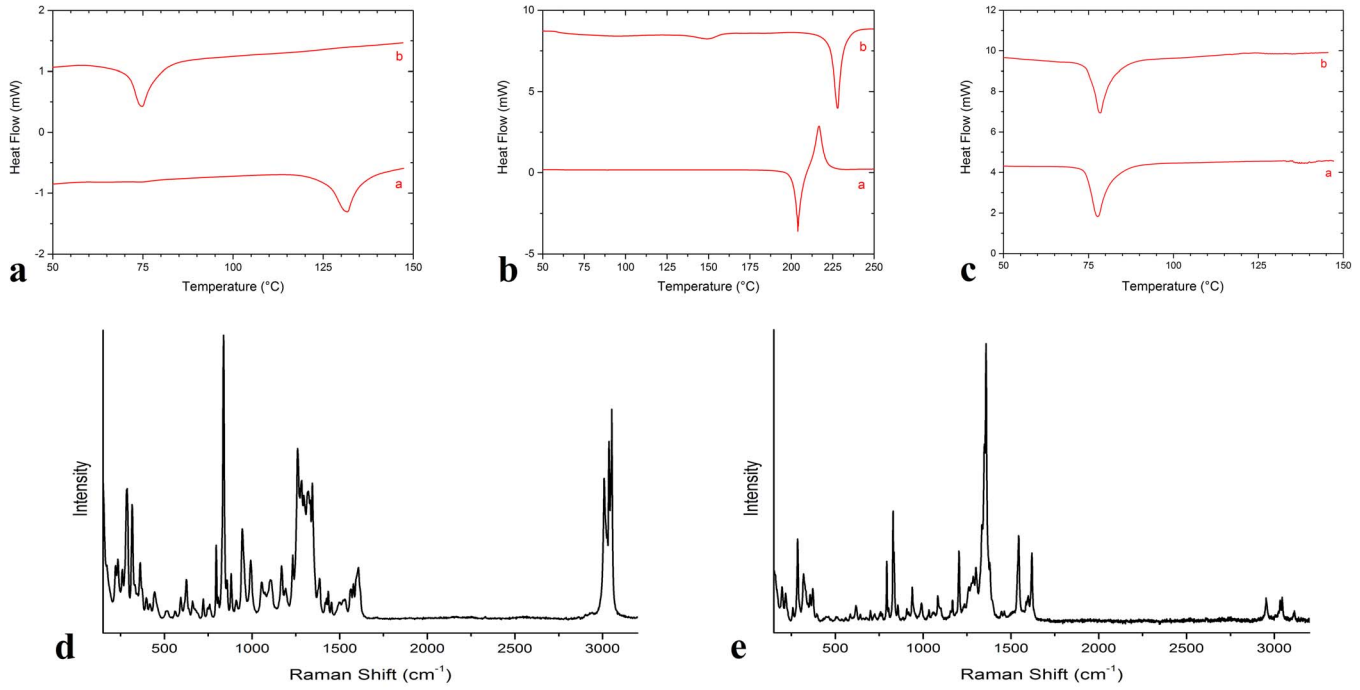

Figure 4 | **Upper part: DSC Curves of the cocrystals and semi-crystalline mixtures.** (a), TNT/CL-20 1 : 1, (b), Caffeine/Oxalic acid 2 : 1, and (c), TNT/HMX 1 : 1. For each graph, "a" and "b" are the first and the second heating phase, respectively. Heating ramp: 5°C/min. Lower part: Raman spectroscopy of the as synthesized cocrystals. (d), HMX/CL-20 1 : 2, and (e), TNT/CL-20 1 : 1.

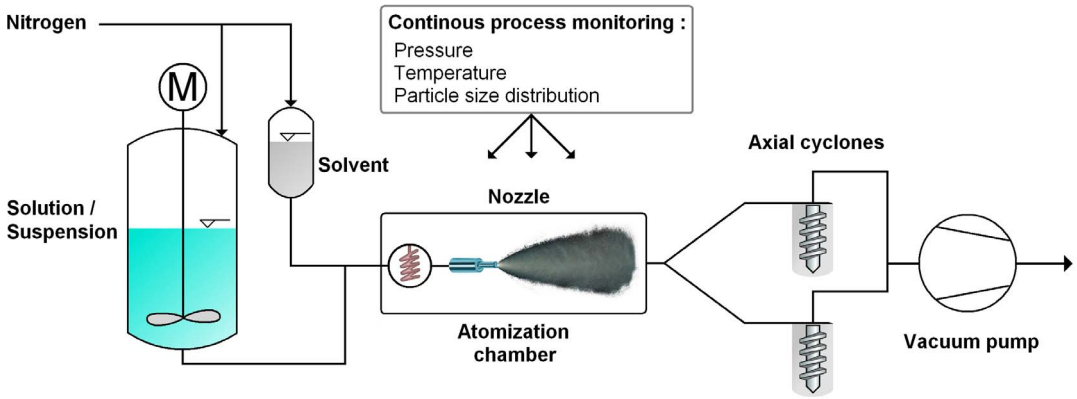

Figure 5 | Process flow chart of the Spray Flash Evaporation process. Drawing created by the authors, software: Gimp 2.8, Inkscape 0.48.5 and Paint 6.3.

cocrystalline nature of this compound. Indeed, after dissociation of the cocrystal and breakage of the bimolecular interactions during the first heating, the pristine compounds crystallized separately during the cooling phase.

The existence of the cocrystal Caffeine/Oxalic acid 2 : 1 was also proven by DSC measurements as the first heating phase evidences a melting onset temperature of 199°C, which is between both melting temperatures of the pure compounds (Fig. 4b). This melting behavior is followed by decomposition of released pure oxalic acid during dissociation of the cocrystal. After cooling, the second heating reveals the melting of the only remaining pure caffeine. In case of TNT/HMX 1 : 1 and 1 : 2 mixtures, the specific melting signal of TNT is already present during the first heating phase, and remains unchanged during the second heating. In fact, this shows that the corresponding sample is a physical mixture of independent TNT and HMX nanoparticles (Fig. 4c).

Raman spectra of the energetic/energetic cocrystalline systems HMX/CL-20 1 : 2 and TNT/CL-20 1 : 1 are given in Figure 4d–e. In 4d the most intense Raman band, at ~860 cm^{-1} exactly fits the value of the sharp vibrational band published from Bolton et al. indicating the successful formation of a HMX/CL-20 cocrystal. The most intense signal within the characteristic fingerprint in 4e (TNT/CL-20 1 : 1) is 1360 cm^{-1} featuring nitro functionalities and exactly matching the value of published results from the same group for micronsized cocrystals slowly grown from ethanolic solution[2]. At higher wavenumbers (~3000 cm^{-1}) a second characteristic regime occurs reflecting vibrational modes of CH – for both systems.

In this letter we demonstrate existence and engineering of hybrid nanoparticles that are structured at the subnanometer level which is evidenced by the identified nano-cocrystals. In the field of energetic materials, cocrystals represent an exceeding interest for further investigations of thermal properties of explosives. Due to decomposition of the cocrystal during the melting phase, the crystallization enthalpy of the pure pristine compounds can be measured. These pure compounds, under normal conditions, would decompose first, during or immediately after the melting process. For medical issues, we demonstrate that continuous engineering of API-based nanococrystals is possible and grams - even kilograms - per hour production rate can be reached for an industrial continuous production of essential cocrystal-based medicaments. This is the first time production rates within the mentioned order were achieved by our method. In the near future, produced cocrystals may also impact a broader variety of domains of applications such as ferroelectrics[23–24], nonlinear response materials[25], and electronic organics[26]. As recent studies have demonstrated the need of nanostructured explosive composites for synthesizing extremely small nanodiamonds by detonation for photonic and quantum applications, energetic nanococrystals used as precursors, may lead to further breakthroughs[27–31].

Methods

The nano-cocrystals and nanocomposites were all prepared by means of the Spray Flash Evaporation technique[20–22], a process that allows continuous preparation of numerous thermosensitive nanomaterials and compositions within a single processing step (Fig. 5). As the name implies, the basis for this process is the flashing behaviour of superheated liquids that are subject to a sudden pressure drop. The substances intended to be crystallized are dissolved in a low boiling solvent. In general, most liquids with a boiling point below 60°C are suited for this process, covering a wide range of common solvents. Using an overpressure of 40 to 60 bars, the solution is atomized into an evacuated atomization chamber by means of a heated hollow cone nozzle. The pressure in the atomization chamber is kept constant at 5 mbar using a 35m^3/h vacuum pump. Due to a sudden pressure drop, the thermodynamic equilibrium displaces and the superheated solution becomes thermodynamic unstable. To regain its thermodynamic stability the excess thermal energy converts into latent energy, causing the ultra fast evaporation of the solvent and inducing crystallization of the solute. This sudden pressure drop is accompanied by a strong temperature drop of almost 200°C (in fact, from 160°C nozzle temper-

Table 1 | Crystallization experimental processing conditions. Caf: caffeine, Ox: oxalic acid, Glu: glutaric acid

	Caffeine/Oxalic acid	Caffeine/Glutaric acid	TNT/CL20	HMX/CL20	TNT/HMX	TNT/HMX
Molar ratio	2 : 1	1 : 1	1 : 1	1 : 2	1 : 1	1 : 2
Solvent	acetone	acetone	acetone	acetone	acetone	acetone
Masses (g)	Caf:3,5g Ox:0,8g	Caf:4,8g Glu:3,2g	TNT:2,4g CL20:1,2g	HMX:2,7g CL20:8,0g	TNT:3,4g HMX:4,5g	TNT:2,2g HMX:5,7g
Solute conc. (w-%)	1,0	2,0	1,0	2,7	2,0	2,0
Vol. Solution (mL)	500	500	460	500	500	500
Nozzle temp. (°C)	160	160	170	170	160	160
Cyclone temp. (°C)	80	80	50	80	80	80
Nozzle dia. (μm)	60	60	60	60	60	60
Pressure (bar)	40	40	40	50	50	40
Duration (min)	68	56	60	44	41	62
Product (g)	2,77	5,13	1,59	4,93	5,35	4,85
Yield (%)	64,7	64,1	43,8	46,1	67,8	60,6

ature to −30°C nearby the spray outlet[20]), having a protective effect on the nanoparticles and preventing their further growth. Because of low thermal load - acting on the solute - the process can be adapted to a broad product range. Continuous separation of nanoparticles is achieved by in parallel mounted axial cyclones, enabling the extraction of the product from the running system. Further drying experiments exclude residual solvent in the space of our product. The variable process parameters used for the preparation of the cocrystals and the physical mixtures, are listed below (Tab. 1).

AFM patterns were recorded using a MultiMode Nanoscope IV configuration from the Bruker Metrology Group (Santa Barbara, USA) that is equipped with a Bruker 'RTESP' (Rotated Tip Etched Silicon Probe) AFM probe. This probe has a silicon cantilever with a length of 125 mm, a width of 35 mm and a thickness of 4 mm. The tip has a curvature radius of about 10 nm. Raman spectroscopy was conducted with a Renishaw (Gloucestershire, UK) inVia Raman microscope and a 514 nm laser. XRD scans in Bragg-Brentano geometry were performed on a Bruker AXS Advance D8 (Karlsruhe, Germany) X-ray diffractometer using Cu Kα radiation ($\lambda_{K\alpha} = 1.54$ Å) at an acceleration voltage of 40 kV and 40 mA, operating current. DSC was performed on a Q1000 from TA Instruments (New Castle, USA).

1. Brittain, H. G. Cocrystal systems of pharmaceutical interest: 2011. *Cryst. Growth Des.* **12**, 5823–5832 (2012).
2. Bolton, O. & Matzger, A. J. Improved stability and smart-material functionality realized in an energetic cocrystal. *Angew. Chem. Int. Ed.* **50**, 8960–8963 (2011).
3. Shan, N. & Zaworotko, M. J. The role of cocrystals in pharmaceutical science. *Drug Discov. Today* **13**, 440–446 (2008).
4. Sekhon, B. S. Pharmaceutical cocrystal – a review. *Ars Pharm* **50**, 99–117 (2009).
5. Gao, Y., Zu, H. & Zhang, J. Enhanced dissolution and stability of adefovir dipivoxil by cocrystal formation. *J. Pharm. Pharmacol.* **63**, 483–490 (2011).
6. Bethune, S. J., Schultheiss, N. & Henck, J. O. Improving the poor aqueous solubility of nutraceutical compound pterostilbene through cocrystal formation. *Cryst. Growth Des.* **11**, 2817–2823 (2011).
7. Yu, Z. Q., Chow, P. S., Tan, R. B. H. & Han Ang, W. Supersaturation control in cooling polymorphic co-crystallization of caffeine and glutaric acid. *Cryst. Growth Des.* **11**, 4525–4532 (2011).
8. Trask, A. V., Motherwell, W. D. S. & Jones, W. Pharmaceutical co-crystallization: engineering a remedy for caffeine hydration. *Cryst. Growth Des.* **5**, 1013–102 (2005).
9. Henning, G. F. DRP-patent N° 104280 (1898).
10. Landenberger, K. B., Bolton, O. & Matzger, A. J. Two isostructural explosive cocrystals with significantly different thermodynamic stabilities. *Angew. Chem. Int. Ed.* **52**, 1–5 (2013).
11. Thottempudi, V. & Shreeve, J. M. Synthesis and promising properties of a new family of high-density energetic salts of 5-nitro-3-trinitromethyl-1H-1,2,4-triazole and 5,5'-bis (trinitromethyl)-3,3'-azo-1H-1,2,4-triazole. *J. Am. Chem. Soc.* **133**, 19982–19992 (2011).
12. Lin, H. *et al.* Synthesis and first principles investigations of HMX/NMP cocrystal explosives. *Journal of Energetic Materials* **31**, 261–272 (2013).
13. Bolton, O., Simke, L. R., Pagorai, P. F. & Matzger, A. J. High power explosive with good sensitivity: A 2:1 cocrystal of CL-20: HMX. *Cryst. Growth Des.* **12**, 4311–4314 (2012).
14. Millar, D. I. A. *et al.* Crystal engineering of energetic materials: cocrystals of Cl-20. *CrystEngComm.* **14**, 3742–3749 (2012).
15. Zhang, H. *et al.* Five energetic cocrystals of BTF by intermolecular hydrogen bond and π-stacking interactions. *Cryst. Growth Des.* **13**, 679–687 (2013).
16. Landenberger, K. B. & Matzger, A. J. Cocrystals of 1,3,5,7-tetranitro-1,3,5,7-tetrazacyclooctane (HMX). *Cryst. Growth Des.* **12**, 3603–3609 (2012).
17. Yang, Z. *et al.* Characterization and properties of a novel energetic-energetic cocrystal explosive composed of HNIW (CL-20) and BTF. *Cryst. Growth Des.* **12**, 5155–5158 (2012).
18. Zhang, C. *et al.* Toward low-sensitive and high energetic cocrystal I: evaluation of the power and the safety of observed energetic cocrystals, *CrystEngComm.* **15**, 4003–4014 (2013).
19. Stepanov, V., Anglade, V., Balas Hummers, W. A., Bezmelnitsyn, A. V. & Krasnoperov, L. N. *Propellants Explos. Pyrotechn.* **36**, 240–246 (2011).
20. Risse, B. *et al.* Continuous formation of submicron energetic particles by the flash-evaporation technique. *Chemical Engineering Journal* **203**, 158–165 (2012).
21. Risse, B., Spitzer, D. & Hassler, D. Preparation of nanoparticles by flash evaporation. Patent WO 2013/117671 A1 (2013).
22. Risse, B., Spitzer, D. & Pichot, V. Method of manufacturing nanoparticles by detonation. Patent WO 2013/127967 A1 (2013).
23. Tayi, A. S. *et al.* Room-temperature ferroelectricity in supramolecular networks of charge-transfer complexes. *Nature* **488**, 485–489 (2012).
24. Horiuchi, S. & Tokura, Y. Organic ferroelectrics. *Nat. Mater.* **7**, 357–366 (2008).
25. Marder, S. R., Perry, J. W. & Schaefer, W. P. Synthesis of organic salts with large second-order optical nonlinearities. *Science* **245**, 626–628 (1989).
26. Pan, F. *et al.* A novel and perfectly aligned highly electro-optic organic cocrystal of a merocyanine dye and 2,4-dihydroxybenzaldehyde. *J. Am. Chem. Soc.* **118**, 6315–6316 (1996).
27. Pichot, V., Risse, B., Schnell, F., Mory, J. & Spitzer, D. Understanding ultrafine nanodiamond formation using nanostructured explosives. *Scientific Reports* **3**, 2159 (2012).
28. Aharonovich, I., Greentree, A. D. & Prawer, S. Diamond photonics. *Nature Photon.* **5**, 397–405 (2011).
29. Mochalin, V. N., Shenderova, O., Ho, D. & Gogotsi, Y. The properties and applications of nanodiamonds. *Nature Nanotech.* **7**, 11–23 (2012).
30. Pawlak, R., Glatzel, T., Pichot, V., Spitzer, D. & Meyer, E. Local detection of nitrogen-vacancy centers in an nanodiamond monolayer. *Nano Lett.* **13**, 5803–5807 (2013).
31. Vlasov, I. I. *et al.* Molecular-sized fluorescent nanodiamonds. *Nature Nanotech.* **9**, 54–58 (2014).

Author contributions

D.S. conceived the original idea and D.S. and B.R. directed the research. B.R. synthesized the cocrystals. D.S., B.R., V.P., F.S., M.K. and M.R.S. participated to the characterization of the products. All authors participated to the analysis of the data and discussed the results. D.S. wrote the paper, and all authors provided their feedback. All authors have read and have approved the manuscript.

Additional information

Competing financial interests: The authors declare no competing financial interests.

How to cite this article: Spitzer, D. *et al.* Continuous engineering of nano-cocrystals for medical and energetic applications. *Sci. Rep.* **4**, 6575; DOI:10.1038/srep06575 (2014).